Theoretical and Experimental Analysis of a Continuous-Blade Cutting System for Leafy Vegetables

D. Brown, J. L. Glancey

Abstract. *To address the high costs associated with maintaining current reciprocating cutter bars used for harvesting spinach, a project was initiated to develop a lower-cost bandsaw cutting system. A model of the stresses generated in the saw blade under several loading scenarios was developed and used to evaluate the potential for fatigue failure with different support pulley and blade designs. For hardened steel blades, fatigue failure does not seem likely for pulley diameters equal to or greater than 300 mm. Torsional stiffness of a wide-span blade was modeled and used to determine the critical in-plane feed force exerted by the crop above which the blade will buckle. Laboratory tests with an instrumented bandsaw blade testing apparatus confirmed the predictions from the stability model that the critical forces necessary to induce buckling are low. The effects of blade thickness and tension on stability were examined and indicated that the resistance to buckling could be improved with increasing thickness and tension at the expense of fatigue life. For spans greater than 1.5 m, the blade tension required to prevent buckling was not practical, which suggested that the blade must be supported across the cutting width in order to achieve the required forces for cutting. A prototype bandsaw-type harvester was developed that included a continuous polymer blade guide to prevent blade twisting and buckling. Field capacity averaged 1.6 ha/h, corresponding to a throughput capacity in excess of 26 Mg/ha in spinach grown for processing. In-field recovery measurements and an N-way analysis of variance revealed no significant difference in harvest loss between semi-Savoy and smooth leaf spinach varieties. On average, harvest loss was about 5% of the commercial yield; approximately 1% of this loss was attributed to the harvester cutting mechanism as leaves still attached to the spinach crown. The remaining losses were significantly higher, consisting of loose leaves cut by the bandsaw but not gathered by the intake conveyor.*

Keywords. *Harvesting, Specialty crops.*

Spinach is a crop grown in Delaware, New Jersey, and the eastern shore of Maryland for both fresh market and processing use, and virtually all production is machine harvested. When grown for processing, spinach is planted for three different growing/harvesting periods. Spring crops are planted between 12 March and 20 April and harvested between 20 May and 7 June. Fall crops are planted between 10 August and 2 September and harvested between 20 September and 28 October. Overwinter crops are planted between 1 and 15 October and harvested in the spring. In each case, plantings may be harvested as many as three times, provided the plant crown is not damaged during harvest, sufficient re-growth exists, and only a few plants have started to produce seed.

Spinach is a low-growing, fleshy-leafed annual that forms a heavy rosette of broad, crinkly, tender leaves. Spinach is classified as a very hardy cool-season crop that grows best at a mean temperature of 10°C to 15°C. It does not germinate well in hot weather, and if planted in the late spring when hot weather is approaching, the plant will quickly produce a flower stalk and go to seed after the development of only a few leaves.

Spinach for processing is grown on beds planted with narrow, high-density, precision-seeded rows; beds are typically 1.5 m wide and consist of 5 to 8 rows. Bed configuration is often a function of the harvesting equipment attributes and the width of the cutter on the harvester. Final stands should be 7 to 8 plants per 30 cm, although 10 plants per 30 cm are acceptable. Thinner populations will not only enhance control of foliar diseases because of better air circulation, but also produce larger plants and leaves.

Annually, about 2000 ha of spinach are planted in Delaware and Maryland, and another 2000 ha are planted in New Jersey. Average yield is about 15 Mg/ha. The cash farm income to spinach producers in Delaware was approximately $1.3 million in 2003 (Brown and Glancey, 2006).

Overivew of Current Harvesting Methods

Most growers use towed cutters for harvesting (fig. 1). On-the-go transfer into transport carts is required since harvesters do not have on-board storage for harvested spinach. Carts are unloaded into open transport trailers where the spinach is manually bulk packed by several workers.

The conventional cutting mechanism on these harvesters is a reciprocating blade similar to a sickle bar cutter. As shown in figure 2, the blade slides along guards that form a second surface upon which the spinach stem is sheared.

Submitted for review in October 2006 as manuscript number PM 6716; approved for publication by the Power & Machinery Division of ASABE in January 2007. Presented at the 2006 ASABE Annual Meeting as Paper No. 061139.

The authors are **Darren Brown,** Graduate Student, Department of Mechanical Engineering, and **James L. Glancey, ASABE Member Engineer,** Associate Professor, Departments of Bioresources Engineering and Mechanical Engineering, University of Delaware, Newark, Delaware. **Corresponding author:** James L. Glancey, Departments of Bioresources Engineering and Mechanical Engineering, University of Delaware, 263 Townsend Hall, Newark, DE 19717; phone: 302-831-1179; fax: 302-831-3651; e-mail: jglancey@udel.edu.

Vol. 50(3): 803−813 ISSN 0001−2351

Figure 1. Conventional spinach harvesting in the mid-Atlantic region using a towed cutter and a load-on-the-go transport trailer.

When sharp, the blade and guard provide an effective shearing technique for harvesting spinach that is capable of cutting plants as low a 50 mm above the soil surface. However, because of the sandy, well drained soils used for spinach production, the rate of blade and guard wear is very high; often, a cutter bar will need to be replaced within 8 h of operation. Since the blade consists of as many as 30 double-riveted blade sections, cutter bar repairs require numerous hours of labor per week during the harvesting seasons. In addition, the crank-slider mechanism used to drive the reciprocating blade also requires frequent maintenance, again because of the abrasive soil. As a result, harvesting costs for spinach in the mid-Atlantic are high, averaging more than $300/ha.

Objectives of this Study

To address the high costs associated with maintaining current spinach cutter bars, a project was initiated to develop an alternative, lower-cost cutting method. The advent and growth in popularity of fresh-cut, prepackaged vegetable products has led to an increased need for mechanization for many leafy vegetable crops. Currently, several baby leaf vegetables are harvested in California with bandsaw-type mechanical cutters that sever the crop close to the soil surface (Inman, 2003). This work has clearly shown that a continuous-blade cutter performs very well for small vegetable plants. The focus of the current study is to develop a similar bandsaw cutter for larger leaf, high-yield vegetables like mature spinach plants.

Figure 2. Conventional reciprocating cutter bar used for spinach harvesting.

Design of the Continuous-Blade Cutter

Conceptual View of a Bandsaw Cutter for Leafy Vegetables

Bandsaws are still a common method of cutting in a number of industries worldwide, including metalworking, forestry, food, and agriculture. These simple devices are relatively inexpensive, versatile, and easy to maintain. Several different bandsaw configurations have been effectively analyzed and used to cut a number of materials, including steel (Henderer et al., 1996), aluminum (Gendraud et al., 2002), wood (Hutton and Taylor, 1991), food (Saravacos et al., 2003), and farm crops (Kepner, 1959).

Figure 3 illustrates the basic arrangement of a large-span bandsaw cutting system. A scalloped steel blade is supported by a four-pulley system; one of the pulleys is driven by a motor, and the others are idlers. For this study, to provide adequate clearance for an intake conveyor, a four-pulley configuration is examined; however, the analysis developed herein applies to other pulley arrangements as well. Each pulley is mounted on a steel shaft, and the cantilevered shafts are supported by two flange bearings mounted to the support frame. The wide-span system illustrated in figure 3 is highly susceptible to blade deflections and instabilities resulting from in-plane forces exerted by the work (crop) on the blade. The goal of this research was to understand the factors affecting blade life and stability, and develop techniques to mitigate undesirable blade behavior to ensure high-quality, consistent cutting.

Review of Continuous-Blade Cutting Technology

The design and performance of bandsaw blades have been examined extensively through both theoretical analysis and experimental studies. A review of the stresses generated in bandsaw blades is provided by Gendraud et al. (2002), indicating that support pulley diameter and blade thickness have a pronounced effect on blade stresses. The effect of roll tensioning has been found to generate significant residual compressive stresses as well as induce torsional buckling and vibration (Wang and Mote, 1994a, 1994b, 1994c). The effect of saw teeth on blade stress has also been examined and found to be significantly influenced by tooth geometry (Andersson, 2001).

An additional objective in bandsaw research has been to understand the dynamic characteristics of the blade and the resulting performance while cutting. The usual approach is to model the blade as an axially moving beam that vibrates in the lateral (transverse) as well as in-plane directions (Ulsoy and Mote, 1978; Lengoc and McCallion, 1995a, 1995b,

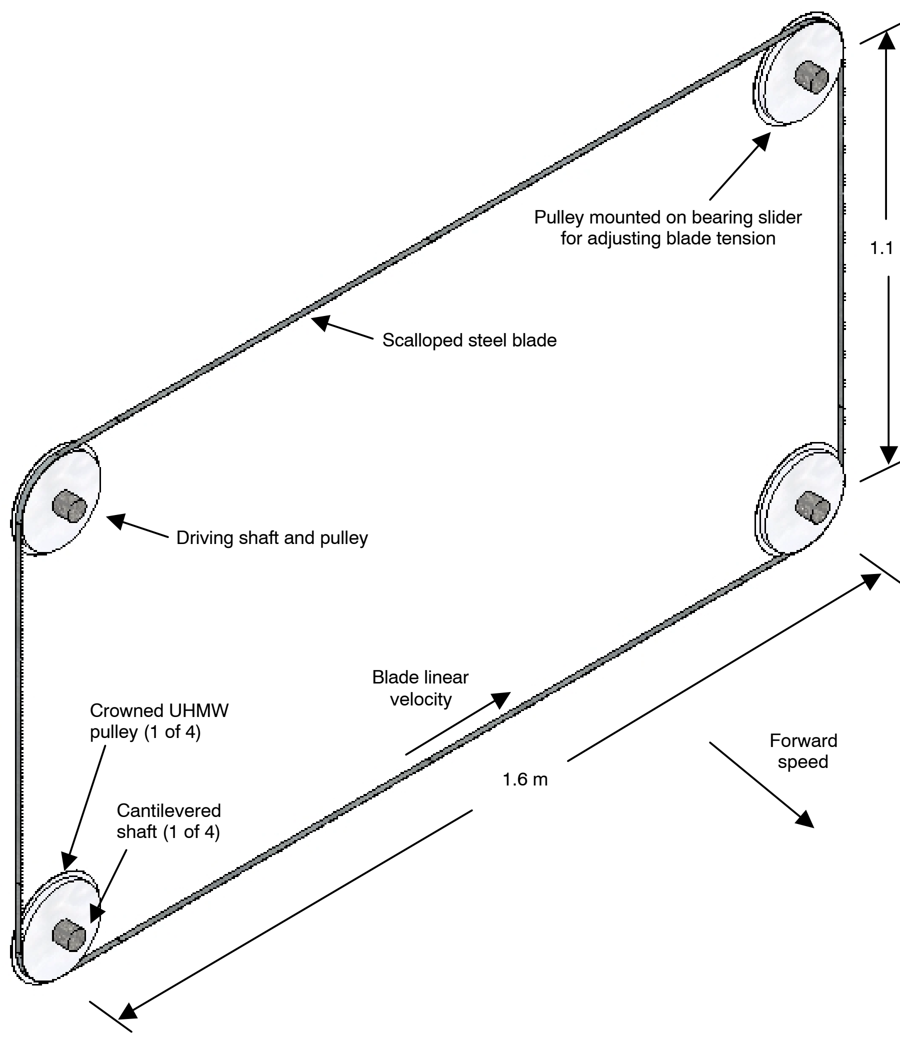

Figure 3. Conceptual view of a bandsaw cutter for spinach grown on 1.5 m beds.

1995c). Treating the blade as a string yields fundamental natural frequencies that have been shown to be lower than the frequencies observed in practice, but are useful as a design guide (Wang and Mote, 1994a). Lateral vibration characteristics are an especially important attribute of blades; improper matching of the tooth passing frequency and the blade natural frequencies can result in poor cut quality. In wood processing, this phenomenon is known as washboarding in which a rough, periodic pattern appears on the cut surfaces (Orlowski and Wasielewski, 2006). Recent studies have shown that a stochastic, on-line, detection methodology can be used to sense and mitigate washboarding by manipulating blade cutting speed (Nanfeng et al., 2001).

The effects of cutting force on dynamic blade behavior have been studied and found to significantly influence tool position and wear (Andersson et al., 2001a, 2001b). A model for the bandsaw frame has also been developed and used to examine the effects of the support structure frame on blade performance (Wojnarowskia and Adamiec-Wójcikb, 2005).

In addition to the detrimental effects associated with transverse blade vibration, blade instabilities in which large blade deflections (both lateral and torsional) develop can also limit performance and reduce blade life. This issue is of particular concern for large-span bandsaws where the unsupported blade length exceeds 1 m. However, no closed-form solution exists to describe the resistance of a wide-span blade to large deflections and buckling. In the analysis that follows, the forces acting on a blade cutting spinach are estimated, and a model of the buckling resistance of wide-span blades is formulated.

Analysis of Blade Stability and Fatigue

Feed Force

The primary force acting on the blade is the horizontal reaction by the crop. By using the impulse-momentum principle and analyzing the mass flow into the harvester as an open system, the total feed force exerted on the blade by the crop can be estimated. Assuming the crop mass flow and harvester forward velocity are constant, the momentum into and out of the system is conserved and the momentum change can be written as:

$$\dot{p} = F - \dot{m}v = 0 \tag{1}$$

where $\dot{p}$ is the momentum change, $\dot{m}$ is the mass flow rate into the harvester, v is the forward speed, and F is the horizontal force exerted on the blade by the cut crop.

The mass flow rate is a function of the harvester forward speed, blade width, and crop yield, and can be computed as:

$$\dot{m}_c = y_c wv \tag{2}$$

where y_c is the crop yield, and w is the harvester cut width. Combining equations 1 and 2 and solving for F gives:

$$F = y_c wv^2 \tag{3}$$

Equation 3 can be used to predict the horizontal (in-plane) force exerted on the blade to change the momentum of the crop; figure 4 contains force estimates at various forward speeds for a harvester width (w) of 1.6 m and crop yields (y_c) of 10 and 20 Mg/ha.

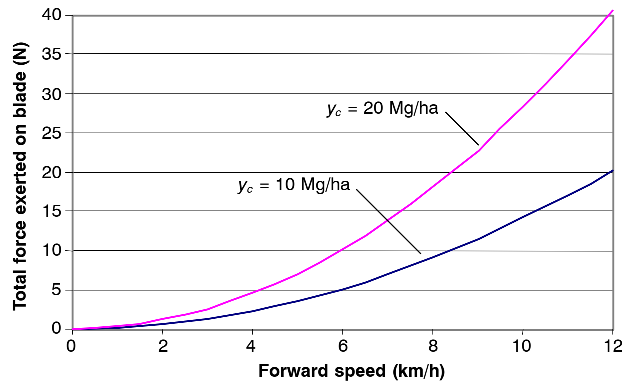

Figure 4. Effects of forward speed (v) and crop yield (y) on the horizontal feed force (F) exerted on the blade by the crop during cutting.

Blade Stiffness and Stability

Given the long, unsupported 1.6 m blade span illustrated in figure 3, poor performance and eventual blade failure resulting from excessive deflection were concerns. As a result, the relation between blade geometry and torsional stiffness was examined. For an unsupported bandsaw blade, the stiffness can be modeled as a long, thin beam (or plate) and expressed as:

$$k = \frac{bc^3G}{3L} \tag{4}$$

where k is the blade torsional stiffness, b is the long cross-sectional dimension (width), c is the short cross-sectional dimension (thickness), G is the shear modulus, and L is the unsupported length (Timoshenko and Goodier, 1970).

An analysis of the effect of the in-plane feed force on the torsional stability of a thin blade can be useful in determining the critical feed force that induces twisting-like buckling phenomena. If this force is exceeded, the blade will undergo large torsional deflections that could result in poor cutting, blade wandering, and eventual failure. To develop a relationship between feed force and blade buckling, the following assumptions are made: deflection angles are considered small, and the blade is considered to be a homogeneous, elastic, isotropic material. Referring to figure 5, it is assumed that the blade is twisted from its equilibrium (horizontal) position by a force (P) exerted on the blade, and this force is sufficient to keep the blade at an angle of twist (θ) against a restoring moment (M) exerted by the blade. The restoring moment consists of two components. The first can be computed by treating the blade as a twisted narrow rectangular cross-section plate; this restoring moment can be computed from the torsional stiffness in equation 4:

$$M_p = k\theta = \frac{1}{3L} bc^3 G\theta \tag{5}$$

where M_p is the restoring moment of a twisted plate, b is the long cross-section dimension (blade width), c is the short cross-section dimension (blade thickness), G is the shear modulus, and θ is the angle of twist.

In addition, the tension in the blade will also try to restore it to equilibrium, thus contributing to the total restoring moment. Figure 6 shows a twisted blade from the in-feed perspective. Force f represents a restoring force based on the amount that the blade is deflected from the neutral axis; as a result, f varies across the width of the blade (i.e., f is a function

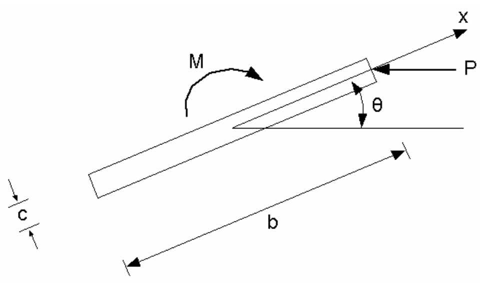

Figure 5. Side view of a twisted blade cross-section.

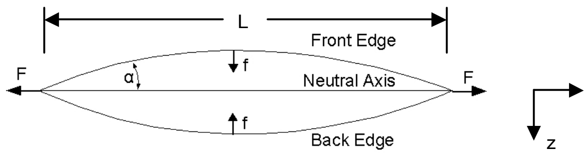

Figure 6. Twisted blade view from feed direction with the front of the blade deflected upwards.

of x). To calculate the restoring moment associated with f, the blade will be divided into infinitesimal slices in the x direction and the couple moment created by f will be integrated along the width b.

Assuming the tension in the blade (T) is uniformly distributed across the blade cross-section, the unit tensile force (F_T) is:

$$F_T = \frac{T}{b} \tag{6}$$

The force (f) produced from a small segment (dx) can then be expressed as:

$$f = 2F_T \sin\alpha dx \tag{7}$$

Note that the factor 2 in equation 7 reflects contributions of the couple from both the left and right sides about the center of the blade. Assuming the deflections are small, the angle α in figure 6 can be expressed as:

$$\alpha = \frac{x\theta}{L/2} \tag{8}$$

Substituting equation 8 into equation 7 yields an expression for force f as a function of x across the blade width:

$$f(x) = \frac{4F_T\theta x}{L}dx \tag{9}$$

This distributed force creates a moment about the neutral axis of the blade; the unit moment can be expressed as:

$$m(x) = \frac{4F_T\theta x^2}{L}dx \tag{10}$$

Integrating across the blade width (b), the restoring moment resulting from the blade tension is:

$$M_T = \int_{\frac{-b}{2}}^{\frac{b}{2}} m(x) = \int_{\frac{-b}{2}}^{\frac{b}{2}} \frac{4F_T\theta x^2}{L}dx \tag{11}$$

or

$$M_T = \frac{4T\theta b^2}{9L} \tag{12}$$

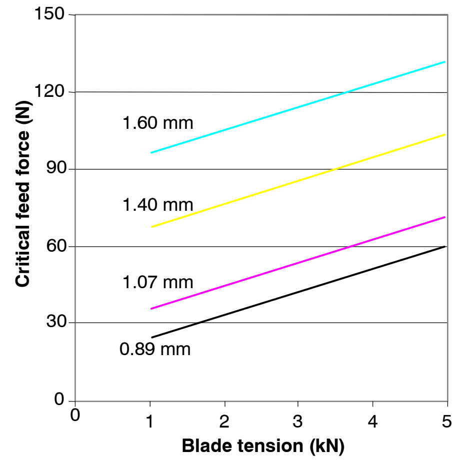

Figure 7. Critical feed force that would induce blade twist as function of blade tension for four different blade thicknesses.

Combining equations 5 and 12, we obtain a final expression for the total restoring moment exerted by the blade:

$$M = \frac{1}{3L}bc^3G\theta + \frac{4T\theta b^2}{9L} \tag{13}$$

Assuming the feed force is sufficient to maintain the angle θ, the moment created by P must be equal and opposite to M. Therefore, the critical load to induce blade twisting can be expressed as:

$$P_{cr} = \frac{2}{3L}c^3G + \frac{8Tb}{9L} \tag{14}$$

Figure 7 contains values of critical feed load as a function of blade tension for four different commercially available blade thicknesses. These results suggest that even for relatively large values of blade tension, the resistance to blade twisting and buckling is low, especially for the thinner blades. Comparison of these critical values to the feed force estimates in figure 4 indicates that the thinnest blade (c = 0.89 mm) will not provide sufficient torsional resistance to prevent blade buckling. As a result, all subsequent analysis will use a blade thickness of c = 1.07 mm.

Fatigue Analysis of the Blade

The effects of blade and pulley geometries on fatigue life were also examined. Stresses in the blade result from both blade tension and bending around support pulleys and can be expressed at a point A on the blade surface as:

$$\sigma_A = \sigma_b + \sigma_t \tag{15}$$

where σ_A is the total stress at point A, σ_b is the stress resulting from blade bending around a pulley, and σ_t is the stresses induced by blade tension.

Bending stress occurs when point A is passing around a pulley and can be calculated using the following expression that relates blade and pulley geometry to peak bending stress:

$$\sigma_b = \frac{Ec}{(2R+c)(1-\upsilon^2)} \tag{16}$$

where E is the elastic modulus, R is the radius of the pulley, and υ is Poisson's ratio (Gendraud et al., 2002). This stress is cyclic in nature and is zero when point A is traveling between pulleys. The tensile stress at point A was assumed constant

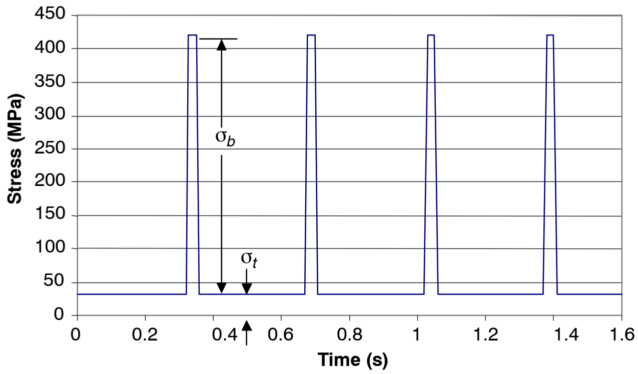

Figure 8. Blade stress during one blade cycle for c = 1.07 mm and the cutter geometry illustrated in figure 3. The blade velocity is 12.5 m/s.

throughout the blade cycle and modeled using the expression:

$$\sigma_t = \frac{T}{cb} \tag{17}$$

By examining point A on the outside surface of the blade, where stress will be maximum, the stress diagram shown in figure 8 was computed for one blade cycle for the geometry shown in figure 3 (b = 25 mm, and c = 1.07 mm). Other blades will have a similar profile, but thicker blades will be subjected to higher bending stress and lower tensile stress, while thinner blades will be subjected to a lower bending stress and a higher tensile stress.

To determine the potential for fatigue failure of the blade, hardness testing was performed on several commercial blade samples to determine the approximate ultimate tensile strength. The hardness was found to be 43 HRC (±1 HRC), which corresponds to an ultimate tensile strength of about 1290 MPa and yield strength of approximately 800 MPa. Using these values, a modified Goodman diagram was constructed and used to plot mean and alternating stresses for four commercially available blade thicknesses (fig. 9).

The mean stress shown figure 9 was calculated using two different methods. Method 1 assumes the mean stress to be the true time-weighted average stress acting on the surface element for one cycle as the element travels around the blade path, and can be computed as:

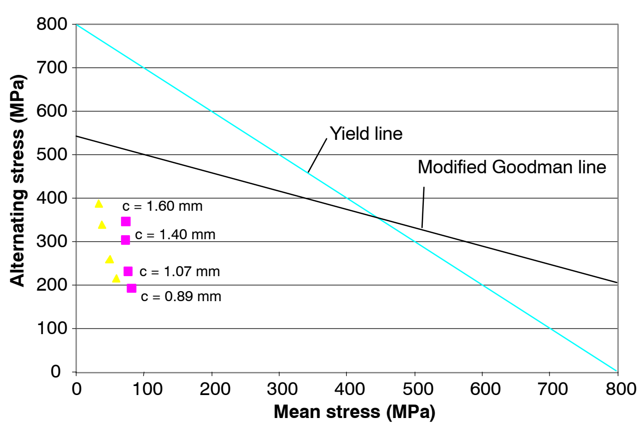

Figure 9. Modified Goodman diagram and computed stresses for four different blade thicknesses. The squares are the stresses predicted using the mean stress calculation from equation 18, and the triangles were computed using equation 19.

$$\sigma_{m_1} = \left(\frac{(H_p + L_p) - \frac{\pi}{2}D}{H_p + L_p} \right) \sigma_T + \left(\frac{\frac{\pi}{2}D}{H_p + L_p} \right) \sigma_B \tag{18}$$

where D is the pulley diameter, L_p is the horizontal distance between pulley centers, and H_p is vertical distance between pulley centers. This method assumes that blade speed is constant over time; therefore, the mean stress depends only on the bandsaw system geometry. Method 2 assumes that the contribution of the bending stress to the time-weighted mean stress is small, which is true for:

$$\frac{D}{H_p + L_p} << 1$$

With this assumption, the mean stress for this method can be approximated as:

$$\sigma_{m_2} \cong \sigma_T \tag{19}$$

The results in figure 9 indicate that all blade thicknesses would not fail from fatigue, since all points lie below the yield and modified Goodman lines. Since the magnitude of the bending stress will not change over time, the safety factors for each blade thickness can be computed from the horizontal distance of each stress point in figure 9 from the modified Goodman line (Shigley et al., 2004). The resulting safety factors are provided in table 1, and as expected, increasing blade thickness decreases the safety factor. For pulley diameters of 225 mm and smaller, fatigue failure is likely for the thicker blades. It should also be noted that for large-span bandsaw configurations, there is a minor but insignificant effect between the two methods used to estimate the mean stress component.

Instability from Slippage Between the Drive Pulley and Blade

To assess the potential for slippage between the blade and the drive pulley, the amount of force that could be transmitted from the drive roller to the blade without losing traction was examined. Using the relationship for a flat-belt drive train, the amount of torque transmitted can be calculated based on blade tension, contact angle, pulley size, and the friction factor between the blade and the pulley (Shigley et al., 2004). The resulting expression for transmitted torque is:

$$T_d = \frac{TDe^{f_f \phi} + 1}{e^{f_f \phi} - 1} \tag{20}$$

where T_d is the allowable drive torque, f_f is the coefficient of friction between the two surfaces, and ϕ is the contact angle between the blade and pulley. Assuming f_f = 0.3 for a polyethylene drive pulley and steel blade (MatWeb, 2005), the relationship between blade tension and the corresponding potential drive torque was computed and is shown in figure 10. Given a pulley diameter of 300 mm, the corresponding force that the blade can exert to shear the crop can be computed. For example, given a blade tension of 1 kN, the allowable drive torque will be 185 N-m, which corresponds to a maximum shear force of 1.2 kN. This suggests that relatively little blade tension is required to generate high cutting forces and still prevent pulley slippage. It should be noted that the actual force required to sever spinach stems is unknown, but the

Table 1. Safety factors corresponding to the stress values plotted in figure 9.

Blade Thickness (mm)	Mean Stress Calculated Using:	
	Equation 18	Equation 19
0.89	2.55	2.48
1.07	2.24	2.08
1.40	1.66	1.53
1.60	1.40	1.34

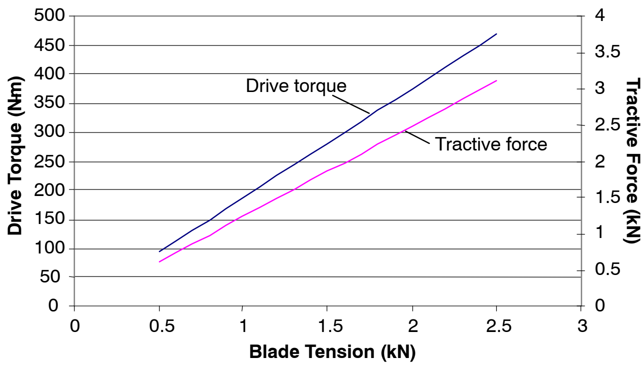

Figure 10. Allowable drive torque and corresponding tractive force generated by the bandsaw blade for various blade tensions. Values were computed using ϕ = 90° and D = 300 mm.

high tractive force values predicted in figure 10 indicate that the bandsaw should be able to generate shear forces sufficient for cutting.

Summary of Analysis

The analysis in the preceding sections suggests that long-span bandsaw systems utilizing commercially available steel blades are not likely to suffer from fatigue failure for pulley diameters of at least 300 mm. The tractive forces needed to transmit power from a drive pulley to the blade can be achieved with relatively little blade tension and should not result in slippage between the pulley and blade. In addition, tractive forces are very high and should be sufficient for shearing plant stems.

However, the ability of long-span blades to resist the feed force exerted during cutting is poor, and will likely limit performance for many materials and applications. High blade tension requirements needed to stabilize deflections would not be practical, and would likely lead to blade failure. To confirm the stability problem predicted with equation 14, experiments to study blade buckling and measure critical feed force were conducted and are presented in the following section.

Laboratory Measurement of Blade Stability

Apparatus for Measuring Blade Stability

To validate the stability analysis described previously, experiments were conducted to measure critical feed force for commercially available blades under different tension loads and spans. A testing apparatus was fabricated that allowed for the direct application and measurement of a feed force (P) on a stationary, long-span bandsaw blade. As illustrated in figure 11, four pulleys were arranged to provide a configuration similar to that illustrated in figure 3. The lower right pulley

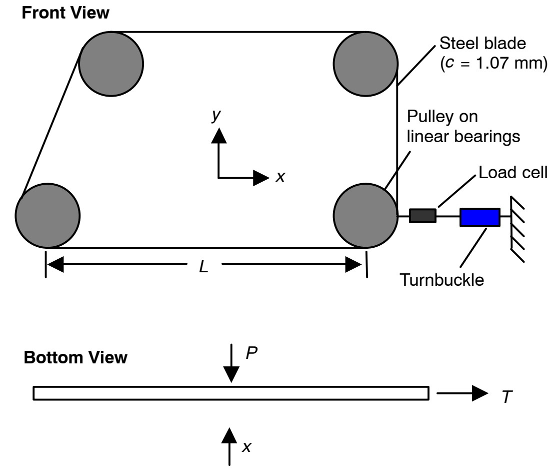

Figure 11. Test apparatus and measured parameters for the blade stability experiments: T = blade tension; P = applied feed force, and L = span length (adjustable from 1.5 to 3.0 m).

was mounted on linear bearings to provide free movement in the x direction and no movement in the y direction. A 13.4 kN load cell and turnbuckle were attached to this pulley and used to apply and measure a horizontal (tension) force acting on the blade. The blade span (L) was adjustable from 1.5 to 3.0 m. Once the span was set and the blade tension adjusted to the desired value, a second load cell (220 N capacity) was used to apply a force (P) in the x direction at the center of the blade (i.e., at L/2).

Both load cell signals were conditioned using a Vishay model 2110B strain gauge conditioner. Amplified signals were recorded with a National Instruments model 6143 S-Series DAQ card (8 channel, 16 bit, 250 kHz max. sampling rate per channel). A LabView program was written to process and record data at a controlled sampling rate of 1 kHz for all tests.

Results from Stability Experiments

Figure 12 contains a typical applied feed force plot recorded during a test corresponding to a blade tension of T = 1 kN. This data corresponds to L = 1.6 m and c = 1.07 mm. The critical feed force for this test when the blade buckled was 32 N.

Figure 13 summarizes measured critical feed force values for three different blade tensions corresponding to a span of 1.6 m and blade thickness of 1.07 mm. Five replicates are plotted at each blade tension, and the resulting coefficient of

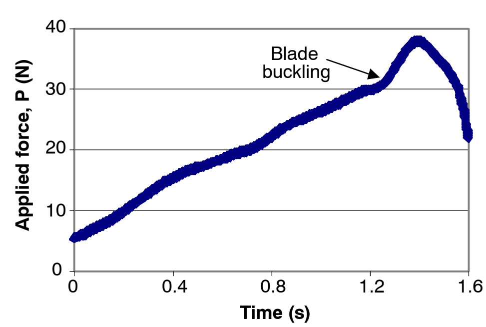

Figure 12. Applied force at the center of the blade during a typical stability test: blade tension (T) = 1 kN, span (L) = 1.6 m, blade thickness (c) = 1.07 mm, and critical feed force (P_{cr}) = 32 N.

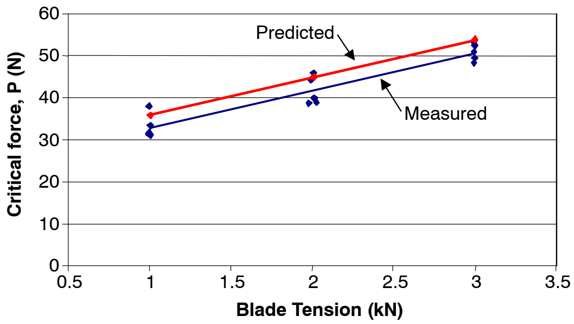

Figure 13. Measured and predicted buckling loads for three different blade tensions for L = 1.6 m and c = 1.07 mm. Predicted values were calculated using equation 14. R^2 = 0.90 for the measured regression line.

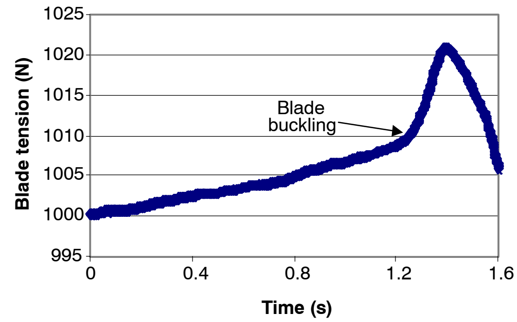

Figure 14. Measured blade tension change for the stability test shown in figure 12.

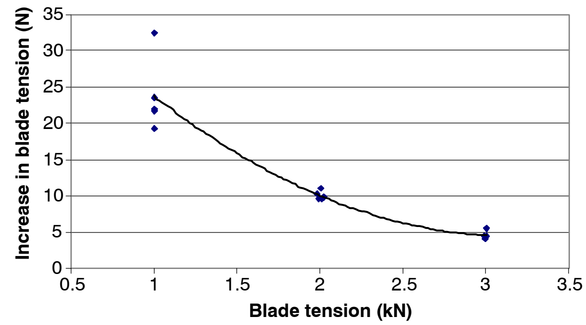

Figure 15. Measured increase in blade tension at the onset of blade buckling corresponding to the data shown in figure 13.

determination (R^2) was 0.90 for the regression line shown on the plot. The line labeled "predicted" in figure 13 represents the critical force values predicted using equation 14. These results validate that the restoring moment that resists blade buckling can be modeled as a function that combines blade torsional stiffness and the additional resistance from blade tension. Furthermore, the ability of long-span, unsupported blades to resist buckling is low and will likely limit performance, even for blades under high tension. For spans greater than 1.5 m, blade performance will be poor, indicating that some type of support is necessary to stabilize the blade, even for moderate feed forces.

Figure 14 is a plot of blade tension during the test illustrated in figure 12 and reveals that blade tension had increased about 21 N at the time of blade buckling; an increase of approximately 2%. Figure 15 contains a summary of the changes in blade tension at buckling for the data presented in figure 13. Overall, blade tension increases were small, averaging about 2% for a 1 kN tension force and 0.12% for a 3 kN tension force. This confirms that changes in blade tension in the presence of feed forces are relatively minor effects that do not significantly increase blade stress or enhance the effective resistance of the blade to twisting and buckling. However, once buckling occurs, blade tension increases significantly, as seen in figure 14.

Prototype Development

A prototype continuous-blade cutter was fabricated using an existing Portaway towed spinach harvester frame. Prior to installation, the reciprocating bar and drive mechanism were removed. The modified cutter, shown in figure 16, utilized a 1.07 mm thick scalloped steel blade and a hydraulic motor to power the drive pulley. Blade span at the bottom (for cutting) was L = 1.6 m. The drive pulley and three idler pulleys were machined from ultra-high molecular weight polyethylene with D = 300 mm; all pulleys included a 2° crown feature to promote proper blade tracking.

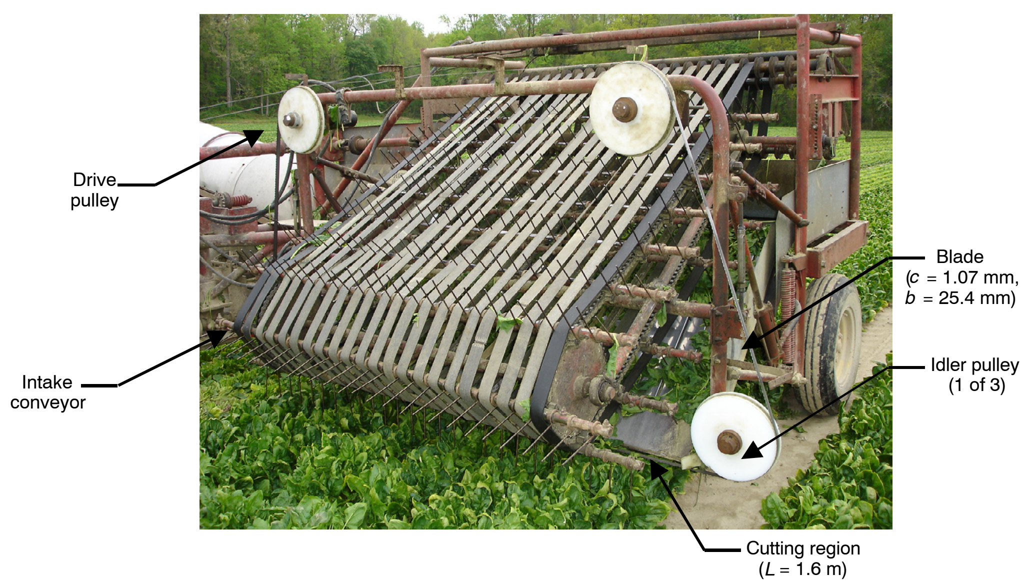

Figure 16. Prototype continuous-blade cutter installed on a Portaway harvester. Safety shields are removed for illustration purposes.

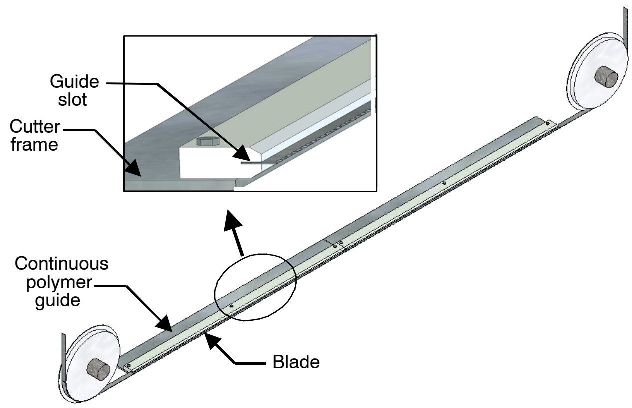

Figure 17. Conceptual view of the blade guide to prevent blade buckling.

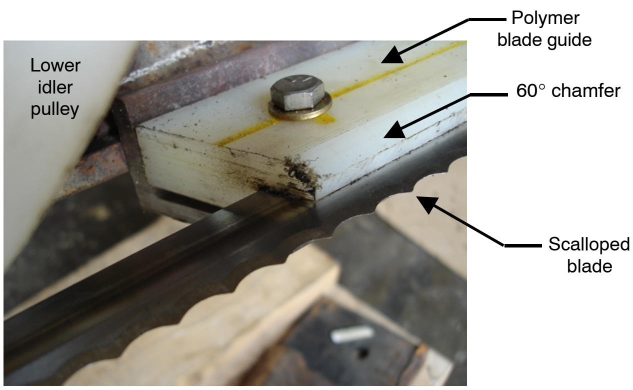

Figure 18. Prototype polymer blade guide installed on the prototype harvester.

Figure 19. Spinach crowns and plant stems after cutting with the prototype continuous-blade harvester. Cutting height was 75 mm.

Preventing Blade Buckling

Stabilizing the blade under high feed forces to prevent buckling and deflection was achieved with a guide that constrained the blade from twisting as well as deflecting upwards. The guide, illustrated in figure 17, was machined from Delrin and included a slot with a depth of 12 mm. The working edge of the blade protrudes from the guide, and the edges of the guide facing the incoming material are chamfered at 60° to promote product flow into the machine. As designed, the guide supports the blade across the entire cutting span and is fastened at 45 cm intervals to the cutter frame, which had previously supported the reciprocating cutter bar. Figure 18 shows the guide installed on the prototype cutter.

Initial field trials with the guide revealed that a relatively large clearance in the guide slot was necessary for the blade to pass freely. If the clearance was less than 0.2 mm, sand particles from the course mid-Atlantic soils used for spinach production became embedded in the slot and caused the blade to seize. For the blade used in this study (c = 1.07 mm), a clearance of 1 mm provided unobstructed performance by allowing larger sand particles to pass through the slot with the blade.

Field Tests

Using the blade guide design shown in figure 17, field tests were conducted in the spring and fall of 2005 and the spring of 2006 in Greenwood (Delaware) and Bridgeton (New Jersey). Recovery and throughput were measured for two spinach varieties: Tyee (semi-Savoy, large leaf), and Vivos (smooth, large leaf). Spinach was grown on 6 row, 1.5 m beds in a commercial spinach production system, and tests were performed on the first and second harvests for most plantings.

Quality of Cut

Figure 19 shows a typical view of spinach crowns and plant stems after cutting with the continuous-blade cutter. A cut height of 75 mm was consistently achieved, and could be controlled with adjustable skids behind the blade. Examination of the cut stems in figure 19 indicates that cut quality was excellent, and that stem failure was the result of blade shearing and not tensile failure (i.e., pulling of the stems to induce failure). Limiting tensile loads in the stem is important for maintaining the integrity of the spinach crown for re-growth.

Throughput and Harvest Recovery Measurements

A summary of field capacity measurements is provided in table 2. Ground speed was adjusted to achieve the maximum throughput capacity without plugging the harvester. True forward speed of the harvester was then determined by measuring the time to traverse 20 m while harvesting. Harvester forward speed averaged 8.9 km/h, corresponding to an average field capacity of 1.62 ha/h. Spinach yield for the 30 ha field used for final testing was 16.4 Mg/ha; the resulting throughput capacity of the bandsaw cutter averaged 26.6 Mg/h.

Field loss measurements were taken randomly throughout the field. Each sampling area was 5.8 m^2 in size (3.04 ×

Table 2. Summary of field capacity measurements (standard deviations in parentheses).

Performance Metric	Average Value
Ground speed (km/h)	8.9 (0.24)
Spinach yield (Mg/ha)	16.4
Field capacity (ha/h)	1.62 (0.06)
Throughput capacity (Mg/h)	26.6 (0.72)

Table 3. Summary of harvest loss measurements for the pooled variety data and a crop yield of 16.4 Mg/ha.

	Loss (kg/ha)			Loss (% yield)		
	Uncut	Loose	Total	Uncut	Loose	Total
Average	171	709	879	1.1	4.3	4.4
Std. Dev.	48	225	227	0.29	1.37	1.39

1.9 m), and six measurement areas were identified for each variety. Spinach leaf losses were gathered immediately after the harvester passed through a test area. Loose leaves and leaves still attached to the crown were collected separately, and all samples were weighted in the field immediately after collection. Total harvest loss was computed as the sum of the loose and uncut leaf losses.

An analysis of variance (ANOVA) was performed to determine which factors had an effect on total harvest loss. The *N*-way ANOVA routine in Matlab 7.0 was used for the analysis. For a 95% confidence level, spinach variety had no statistically significant effect on either uncut or loose harvest losses. Uncut leaf losses were significantly lower that loose leaf losses by about a factor of 4, indicating that the bandsaw was effectively cutting plant stems, but some cut leaves were not being gathered by the intake conveyor. Losses for the pooled variety data are provided in table 3 and indicate that, on average, total harvest loss was about 5% of yield. Of these losses, about 1% was uncut leaves and the remaining 4% was loose leaves. At a price of \$0.22/kg, this represents an average economic loss of \$193/ha, suggesting that an improved intake system that better retains cut leaves could provide a significant savings for growers.

Conclusions

An analysis of large-span bandsaw cutting systems has been developed and validated. For hardened steel blades, fatigue failure does not seem likely for pulley diameters equal to or greater than 300 mm. Examination of two different methods of estimating the mean blade stress revealed little practical difference between the approximation that the mean stress was equal to the stress resulting from blade tension alone versus a more elaborate weighting technique that accounted for the short durations of high stress while the blade was in contact with the pulleys.

A model of blade stability revealed that relatively low feed forces exerted by the crop could induce excessive blade twist, resulting in a buckling-like phenomenon of the blade. Laboratory tests with an instrumented bandsaw blade testing apparatus confirmed predictions from the stability model that the critical forces necessary to induce buckling were on the order of 30 to 60 N. Measured changes in blade tension in the presence of an applied feed force were small and did not significantly increase stress or enhance the resistance of the blade to twisting and buckling.

A bandsaw-type harvester was developed that included a polymer blade guide to prevent blade twisting and buckling. The prototype was successfully used to harvest 30 ha and two spinach varieties in a commercial production setting. Field capacity exceeded 1.6 ha/h, corresponding to a throughput capacity of more than 26 Mg/ha in spinach grown for processing. In-field recovery measurements and an *N*-way analysis of variance showed no significant difference in harvest loss between semi-Savoy and smooth leaf spinach varieties. On average, harvest loss was about 5% of the commercial yield. Approximately 1% of this loss was attributed to the harvester cutting mechanism as leaves still attached to the plant crown. The remaining losses were significantly higher, consisting of loose leaves not gathered by the intake conveyor.

References

Andersson, C. 2001. Bandsawing: Part III. Stress analysis of saw tooth microgeometry. *Intl. J. Machine Tools and Manufacture* 41(2): 255-263.

Andersson, C., M. Andersson, and J. Stahl. 2001a. Bandsawing: Part I. Cutting force model including effects of positional errors, tool dynamics, and wear. *Intl. J. Machine Tools and Manufacture* 41(2): 227-236.

Andersson, C., J. Stahl, and H. Hellbergh. 2001b. Bandsawing: Part II. Detecting positional errors, tool dynamics, and wear by cutting force measurement. *Intl. J. Machine Tools and Manufacture* 41(2): 237-253.

Brown, D., and J. Glancey. 2006. Analysis of a continuous-blade band-type cutter for leafy vegetables. ASABE Paper No 061139. St. Joseph, Mich.: ASABE.

Gendraud, P., J.-C. Roux, and J. M. Bergheau. 2002. Vibrations and stresses in band saws: A review of literature for application to the case of aluminum-cutting high-speed band saws. *J. Materials Processing Tech.* 135(1): 109-116.

Henderer, W. E., J. R. Holston, and J. D. Boor. 1996. Estimation of cutting forces in band sawing metals. Technical paper. Dearborn, Mich.: Society of Manufacturing Engineers.

Hutton, S. G., and J. Taylor. 1991. Operating stresses in band saws and their effects on fatigue life. *J. Forestry Prod.* 41: 7, 12-20.

Inman, J. W. 2003. Fresh vegetable harvesting. *Resource* 10(8): 7-8.

Kepner, R. A. 1959. Mechanical harvester for green asparagus. *Trans. ASAE* 2(1): 84-87, 91.

Lengoc, L., and H. McCallion. 1995a. Wide bandsaw blade under cutting conditions: Part I. Vibration of a plate moving in its plane while subjected to tangential edge loading. *J. Sound and Vibration* 186(1): 125-142.

Lengoc, L., and H. McCallion. 1995b. Wide bandsaw blade under cutting conditions: Part II. Stability of a plate moving in its plane while subjected to parametric excitation. *J. Sound and Vibration* 186(1): 143-162.

Lengoc, L., and H. McCallion. 1995c. Wide bandsaw blade under cutting conditions: Part III. Stability of a plate moving in its plane while subjected to nonconservative cutting forces. *J. Sound and Vibration* 186(1): 163-179.

MatWeb. 2005. The Online Materials Information Resource. Available at: www.matweb.com. Blacksburg, Va.: Automation Creations, Inc. Accessed 27 June 2005.

Nanfeng, Z., C. Tanaka, T. Ohtani, and H. Usuki. 2001. Automatic detection of washboarding in bandsaws. *J. Wood Sci.* 47(2): 102-108.

Orlowski, K., and R. Wasielewski. 2006. Study washboarding phenomenon in frame sawing machines. *Holz als Roh - und Werkstoff* 64(1): 37-44.

Saravacos, G. D., A. F. Harvey, and A. E., Kostaropoulos. 2003. *Handbook of Food Processing Equipment.* New York, N.Y.: Springer.

Shigley, J. E., C. R. Mischke, and R. G. Budynas. 2004. *Mechanical Engineering Design.* 7th ed. New York, N.Y.: McGraw-Hill.
Timoshenko, S., and J. Goodier. 1970. *Theory of Elasticity.* 3rd ed. New York, N.Y.: McGraw-Hill.
Ulsoy, G. A., and C. D. Mote. 1978. Band saw vibration and stability. *Shock Vibration Digest* 10(11): 3-15.
Wang, J., and C. Mote. 1994a. Analysis of roller-induced residual stresses in bandsaw plates. *J. Sound and Vibration* 175(5): 647-659.
Wang, J., and C. Mote. 1994b. On the divergence buckling of a wide bandsaw plate by roll-tensioning. *J. Sound and Vibration* 175(5): 661-675.
Wang, J., and C. Mote. 1994c. The effect of roll-tensioning on bandsaw plate vibration and stability. *J. Sound and Vibration* 175(5): 677-692.
Wojnarowskia, J., and I. Adamiec-Wójcikb. 2005. Application of the rigid finite element method to modelling of free vibrations of a band saw frame. *Mechanism and Machine Theory* 40(2): 241-258.

NOMENCLATURE

b = long cross-sectional blade dimension (width)
c = short cross-sectional dimension (thickness)
D = diameter of the idler and drive pulleys
E = elastic modulus of the blade
F = horizontal force exerted on the crop to change its momentum during cutting
F_T = tensile force in the blade per unit width
f, $f(x)$ = restoring force based on the amount the blade strip is deflected from the neutral axis
f_f = coefficient of friction between the blade and drive pulley
G = shear modulus of the blade
H_p = vertical distance between pulley centers
L = unsupported blade span
L_p = horizontal distance between pulley centers
k = blade torsional stiffness
M = total restoring moment exerted by the blade resisting torsional deflection
M_p = restoring moment of a twisted plate
M_T = restoring moment resulting from the blade tension
$\dot{m}_c$ = crop mass flow rate into the harvester
$m(x)$ = the unit moment resulting from $f(x)$
$\dot{p}$ = momentum change of the crop
P = in-plane feed force exerted on the blade
P_{cr} = critical feed force that induces blade buckling
R = radius of the blade idler and drive pulleys
R^2 = coefficient of determination
T = blade tension
T_d = allowable drive torque of the driving pulley
v = forward speed
w = harvester width of cut
x, y, z = coordinate system with an origin at the center of the blade
y_c = crop yield
υ = Poisson's ratio of the blade material
ϕ = contact angle of the blade with the drive pulley
σ_A = total stress at a point A on the outside surface of the blade
σ_b = bending stress in the blade
σ_{m_1} = mean stress in the blade computed using equation 18
σ_{m_2} = mean stress in the blade computed using equation 19
σ_t = tensile stress in the blade from blade tension
θ = angle of blade twist